The Plant Cell, Vol. 20: 1775–1785, July 2008, www.plantcell.org © 2008 American Society of Plant Biologists

SCREAM/ICE1 and *SCREAM2* Specify Three Cell-State Transitional Steps Leading to *Arabidopsis* Stomatal Differentiation [W][OA]

Masahiro M. Kanaoka,[a,1] Lynn Jo Pillitteri,[a] Hiroaki Fujii,[b] Yuki Yoshida,[c] Naomi L. Bogenschutz,[a] Junji Takabayashi,[c] Jian-Kang Zhu,[b] and Keiko U. Torii[a,d,2]

[a] Department of Biology, University of Washington, Seattle, Washington 98195
[b] Department of Botany and Plant Sciences, Institute for Integrative Genome Biology, University of California, Riverside, California 92521
[c] Center for Ecological Research, Kyoto University, Otsu, Shiga 520-2113 Japan
[d] Institute for Stem Cell and Regenerative Medicine, University of Washington, Seattle, Washington 98195

Differentiation of specialized cell types in multicellular organisms requires orchestrated actions of cell fate determinants. Stomata, valves on the plant epidermis, are formed through a series of differentiation events mediated by three closely related basic-helix-loop-helix proteins: SPEECHLESS (SPCH), MUTE, and FAMA. However, it is not known what mechanism coordinates their actions. Here, we identify two paralogous proteins, SCREAM (SCRM) and SCRM2, which directly interact with and specify the sequential actions of SPCH, MUTE, and FAMA. The gain-of-function mutation in *SCRM* exhibited constitutive stomatal differentiation in the epidermis. Conversely, successive loss of *SCRM* and *SCRM2* recapitulated the phenotypes of *fama*, *mute*, and *spch*, indicating that *SCRM* and *SCRM2* together determined successive initiation, proliferation, and terminal differentiation of stomatal cell lineages. Our findings identify the core regulatory units of stomatal differentiation and suggest a model strikingly similar to cell-type differentiation in animals. Surprisingly, map-based cloning revealed that SCRM is INDUCER OF CBF EXPRESSION1, a master regulator of freezing tolerance, thus implicating a potential link between the transcriptional regulation of environmental adaptation and development in plants.

INTRODUCTION

Formation of functional patterns in plants and animals requires coordinated differentiation of specialized cell types. Stomata are microscopic valves on the plant epidermis used for efficient gas and water vapor exchange. In *Arabidopsis thaliana*, stomata differentiate from a subset of protodermal cells called meristemoid mother cells (MMCs), which undergo an asymmetric cell division that gives rise to a small, triangular cell called a meristemoid. Meristemoids reiterate asymmetric divisions and produce surrounding nonstomatal cells, which we termed stomatal lineage ground cells (SLGCs; Shpak et al., 2005). Meristemoids eventually differentiate into guard mother cells (GMCs). A GMC undergoes a single symmetric division to produce a pair of terminally differentiated guard cells (Nadeau and Sack, 2002b; Bergmann and Sack, 2007). Most nonstomatal lineage cells differentiate into highly intercalated pavement cells that restrict water loss.

Initial genetic studies revealed the presence of cell–cell signals that coordinate spacing of stomata while restricting their differentiation (Berger and Altmann, 2000; Nadeau and Sack, 2002a, 2002b; Bergmann et al., 2004; Shpak et al., 2005; Bergmann and Sack, 2007; Hara et al., 2007; Wang et al., 2007). Presently, the model suggests that secretion of a putative ligand, EPIDERMAL PATTERNING FACTOR1, creates a cell–cell signal that is perceived in neighboring cells by putative cell surface receptors, TOO MANY MOUTHS (TMM) and three ERECTA family receptor-like kinases (Nadeau and Sack, 2002a; Shpak et al., 2005; Hara et al., 2007). The signal is mediated via a mitogen-activated protein kinase cascade, including YODA, MEKK4/5, and MPK3/6 (Bergmann et al., 2004; Wang et al., 2007). A putative subtilisin, STOMATAL DENSITY AND DISTRIBUTION1, acts upstream of TMM (Berger and Altmann, 2000; von Groll et al., 2002). These components are predicted to constitute extrinsic, inhibitory cell–cell signals that orient the proper site of asymmetric division and restrict stomatal differentiation. Consistently, overexpression of EPF1 or gain of function of the mitogen-activated protein kinase cascade components leads to an epidermis without stomata (Bergmann et al., 2004; Hara et al., 2007; Wang et al., 2007). In addition to these signaling components, an R2R3-type Myb gene *FOUR LIPS* and its redundant paralog *Myb88* are required for restricting the number of GMC's symmetric division (Lai et al., 2005).

Recently, a trio of closely related basic-helix-loop-helix (bHLH) genes, *SPEECHLESS* (*SPCH*), *MUTE*, and *FAMA*, were discovered as intrinsic positive regulators that direct the entry into

[1] Current address: Graduate School of Science, Nagoya University, Nagoya, Aichi 464-8402, Japan.
[2] Address correspondence to ktorii@u.washington.edu.
The author responsible for distribution of materials integral to the findings presented in this article in accordance with the policy described in the Instructions for Authors (www.plantcell.org) is: Keiko U. Torii (ktorii@u.washington.edu).
[W]Online version contains Web-only data.
[OA]Open Access articles can be viewed online without a subscription.
www.plantcell.org/cgi/doi/10.1105/tpc.108.060848

stomatal cell lineage, transition from meristemoid to GMC, and terminal differentiation of guard cells, respectively (Ohashi-Ito and Bergmann, 2006; MacAlister et al., 2007; Pillitteri et al., 2007). Both loss- and gain-of-function phenotypes, as well as their transient expression patterns, support the hypothesis that SPCH, MUTE, and FAMA are necessary and sufficient for driving transcriptional cascades at each regulatory node (Ohashi-Ito and Bergmann, 2006; MacAlister et al., 2007; Pillitteri et al., 2007, 2008). However, it remains unknown what mechanism coordinates the actions of SPCH, MUTE, and FAMA. Given that bHLH transcription factors act as dimers (Murre et al., 1989), it is possible that SPCH, MUTE, and FAMA homodimerize and function at each precursor state. Alternatively, other factors that are broadly expressed within the stomatal cell lineages may associate with SPCH, MUTE, and FAMA to specify the sequential cell fate decisions.

Here, we report the identification of two paralogous proteins, SCREAM (SCRM) and SCRM2, which specify the sequential actions of SPCH, MUTE, and FAMA, allowing protodermal cells to initiate and execute stomatal cell fate. The gain-of-function mutation in *SCRM* caused constitutive stomatal differentiation in the epidermis. Conversely, successive loss of *SCRM* and *SCRM2* recapitulated the phenotypes of *fama*, *mute*, and *spch*, indicating that a gene dosage of *SCRM* and *SCRM2* determines successive initiation, proliferation, and terminal differentiation of stomatal cell lineages. Our map-based cloning revealed that SCRM is INDUCER OF CBF EXPRESSION1 (ICE1), a master regulator of freezing tolerance.

RESULTS

scream-D, a Dominant Mutant with Constitutive Stomatal Differentiation in the Epidermis

To elucidate the mechanism that coordinates sequential cell fate specification steps during stomatal differentiation, we performed

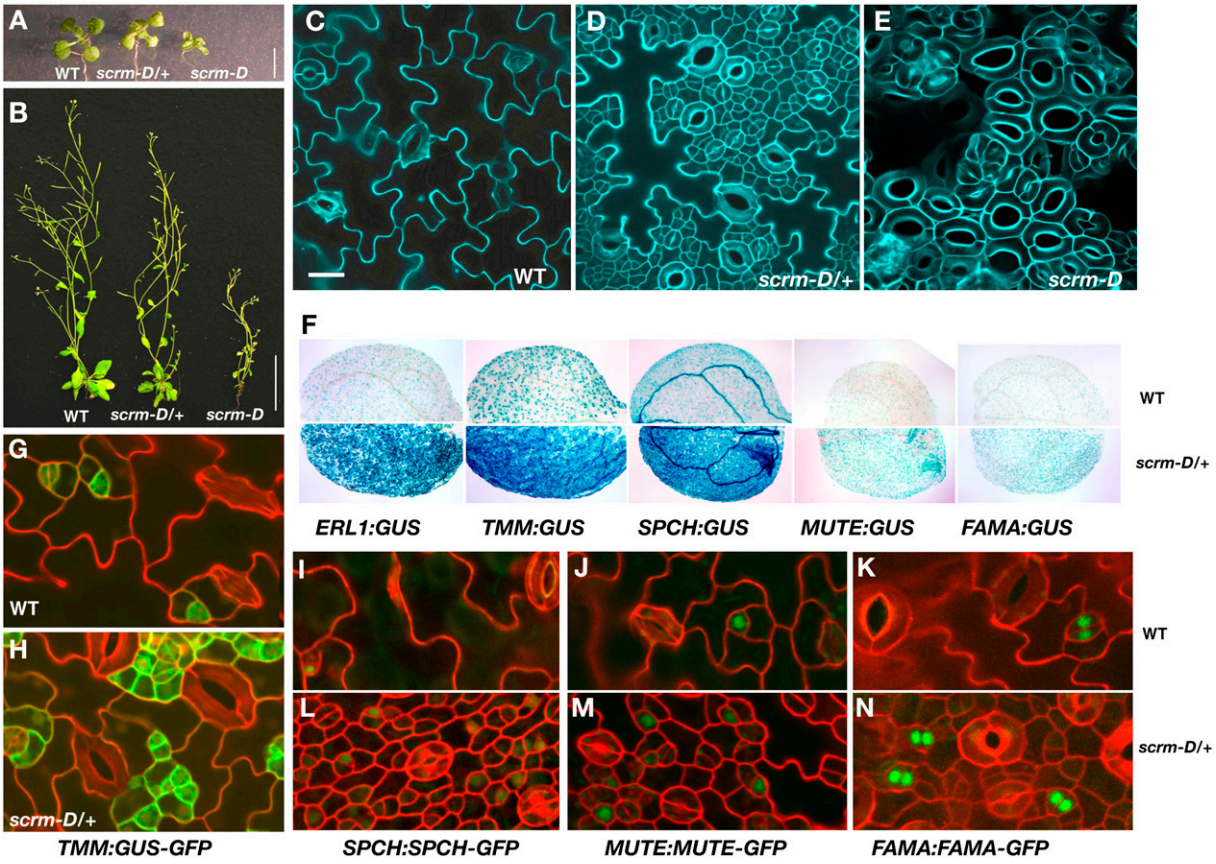

Figure 1. *scrm-D* Triggers Stomatal Differentiation.

(A) Two-week-old seedlings of wild-type, *scrm-D*/+ heterozygous, and *scrm-D* homozygous mutants. Bar = 5 mm.

(B) Six-week-old mature plants of wild-type, *scrm-D*/+ heterozygous, and *scrm-D* homozygous mutants. Bar = 5 cm.

(C) to **(E)** Cotyledon epidermis of the wild type **(C)**, *scrm-D*/+ **(D)**, and *scrm-D* **(E)**. *scrm-D*/+ and *scrm-D* epidermis shows vastly increased stomatal differentiation. Bar = 20 μm.

(F) Cotyledons of the wild type (top) and *scrm-D*/+ (bottom) carrying the reporter construct (from left to right): *ERL1:GUS*, *TMM:GUS*, *SPCH:GUS*, *MUTE:GUS*, and *FAMA:GUS*. *scrm-D*/+ confers increased expression of stomatal cell lineage markers.

(G) to **(N)** Cotyledons of the wild type (**[G]** and **[I]** to **[K]**) and *scrm-D*/+ (**[H]** and **[L]** to **[N]**) carrying *TMM:GUS-GFP* (**[G]** and **[H]**) and translational fusion of SPCH:SPCH-GFP (**[I]** and **[L]**), MUTE:MUTE-GFP (**[J]** and **[M]**), and FAMA:FAMA-GFP (**[K]** and **[N]**). *scrm-D*/+ increases the number of cells expressing stomatal cell lineage markers (GFP; green).

a sensitized genetic screen and isolated a semidominant mutation, *scream-D* (*scrm-D*), that conferred constitutive stomatal differentiation (wild type: *scrm-D*/+: *scrm-D* = 25:46:20; χ^2 = 0.56, P = 0.76). Seedlings and adult plants of the heterozygous *scrm-D*/+ mutant appeared normal aside from wrinkled cotyledons and leaves (Figures 1A and 1B; see Supplemental Figure 1 online). The *scrm-D* homozygous seedlings and adult plants showed severe growth defects with small rosettes, short inflorescences, and reduced fertility (Figures 1A and 1B).

Unlike the wild type, the epidermis of *scrm-D*/+ plants produced highly divided small cells, as well as stomata at high density that were adjacent to each other (Figures 1C and 1D). Strikingly, homozygous *scrm-D* seedlings developed an epidermis solely composed of stomata (Figure 1E). The *scrm-D* plants had severely wrinkled cotyledons and leaves, which often disintegrated due to the absence of interlocking pavement cells (Figure 1; see Supplemental Figure 1 online).

To understand the molecular characteristics of *scrm-D*, we next investigated the promoter activity and expression patterns of stomatal cell-type specific markers. *TMM* and *ERL1* mark stomatal lineage cells with the highest expression in meristemoids, while *SPCH*, *MUTE*, and *FAMA* mark a series of transitional states of stomatal precursors, starting from MMC to immature guard cells (Nadeau and Sack, 2002a; Shpak et al., 2005; Ohashi-Ito and Bergmann, 2006; MacAlister et al., 2007; Pillitteri et al., 2007). Intense reporter β-glucuronidase (GUS) activity was detected in the appropriate cell types of *scrm-D*/+ cotyledons carrying *TMM:GUS*, *ERL1:GUS*, *SPCH:GUS*, *MUTE:GUS*, and *FAMA:GUS* (Figure 1F). Observation at higher resolution revealed that more cells expressed the stomatal lineage marker *TMM:GUS-GFP* (Figures 1G and 1H). The small, highly divided epidermal cells in *scrm-D*/+ showed high accumulation of SPCH:SPCH-GFP (Figures 1I and 1L). Furthermore, the *scrm-D*/+ epidermis overproduced meristemoids and GMCs accumulating MUTE-GFP and FAMA-GFP, respectively (Figures 1J, 1K, 1M, and 1N). These findings suggest that *scrm-D* acts in a gene dosage-dependent manner to vastly increase the number of epidermal cells entering the stomatal lineage.

scrm-D Differentiates Stomata without Reiterative Asymmetric Divisions of Meristemoids

Homozygous *scrm-D* mutant plants differentiate an epidermis solely made of stomata (Figure 1E). To understand how these stomata are generated, we examined the time course of stomatal differentiation in germinating cotyledons of homozygous *scrm-D* mutants using the reporter *TMM:GUS-GFP* (Figure 2; Nadeau and Sack, 2002a). At 1 d after germination, a subset of protodermal cells in wild-type cotyledons expressed *TMM:GUS-GFP* (Figure 2A). These green fluorescent protein (GFP) positive cells were evenly spaced with a rare occasion of two adjacent cells both expressing GFP (Figure 2A). By contrast, the majority of protodermal cells were GFP positive in *scrm-D* seedlings at 1 d after germination (Figure 2B). At 3 d after germination, GFP positive cells underwent cell divisions both in wild-type and *scrm-D* seedlings (Figures 2C and 2D). By 4 d after germination, meristemoids and SLGCs became evident in wild-type epidermis (Figures 2E and 2G). By contrast, stomatal lineage cells in the

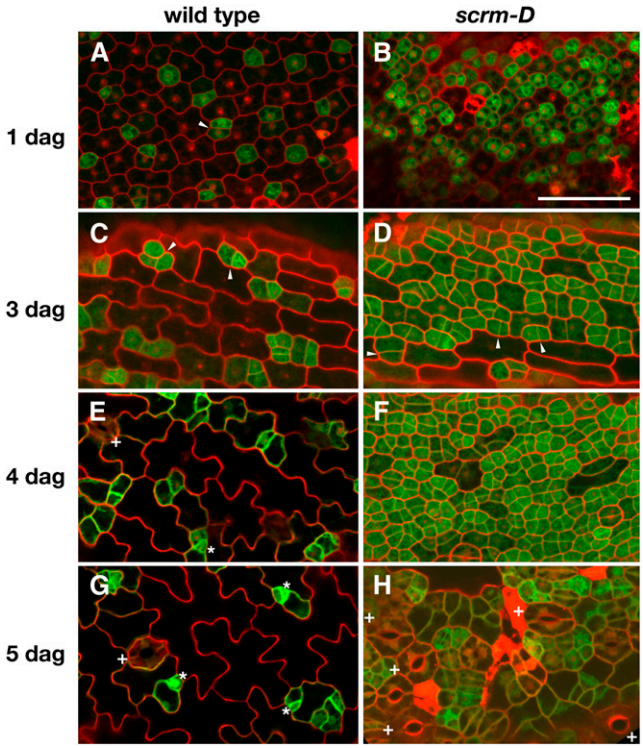

Figure 2. Time Sequence of Stomatal Differentiation in *scrm-D*.

Images of the abaxial epidermis of wild-type and scrm-D cotyledons. TMM:GUS-GFP (green) was used to monitor stomatal lineage cells. Arrowheads, GFP positive cells underwent cell division; asterisks, meristemoids; +, mature stomata. Images were taken under the same magnification. Bar = 50 μm.

(A) Wild-type cotyledon at 1 d after germination (dag).
(B) *scrm-D* cotyledon at 1 d after germination.
(C) Wild-type cotyledon at 3 d after germination.
(D) *scrm-D* cotyledon at 3 d after germination.
(E) Wild-type cotyledon at 4 d after germination.
(F) *scrm-D* cotyledon at 4 d after germination.
(G) Wild-type cotyledon at 5 d after germination.
(H) *scrm-D* cotyledon at 5 d after germination.

scrm-D epidermis kept undergoing cell division and initiated guard cell differentiation without properly establishing the SLGC identity (Figure 2F). At 5 d after germination, many epidermal cells in *scrm-D* differentiated into mature stomata and lost GFP activity (Figure 2H). These observations indicate that in *scrm-D*, epidermal cells differentiate into stomata without reiterating asymmetric cell divisions of meristemoids.

SCRM Likely Acts Immediately Downstream of *SPCH*

The "stomata only" *scrm-D* phenotype is identical to that of ectopic *MUTE* overexpression (Pillitteri et al., 2007). This led us to investigate the genetic interactions of *scrm-D* with *mute*, *fama*, and *spch*. In *mute*, meristemoids arrested and failed to differentiate into GMCs (Figure 3A). *mute scrm-D* double mutants developed an epidermis highly enriched with small, triangular meristemoids, thus greatly exaggerating the *mute* phenotype

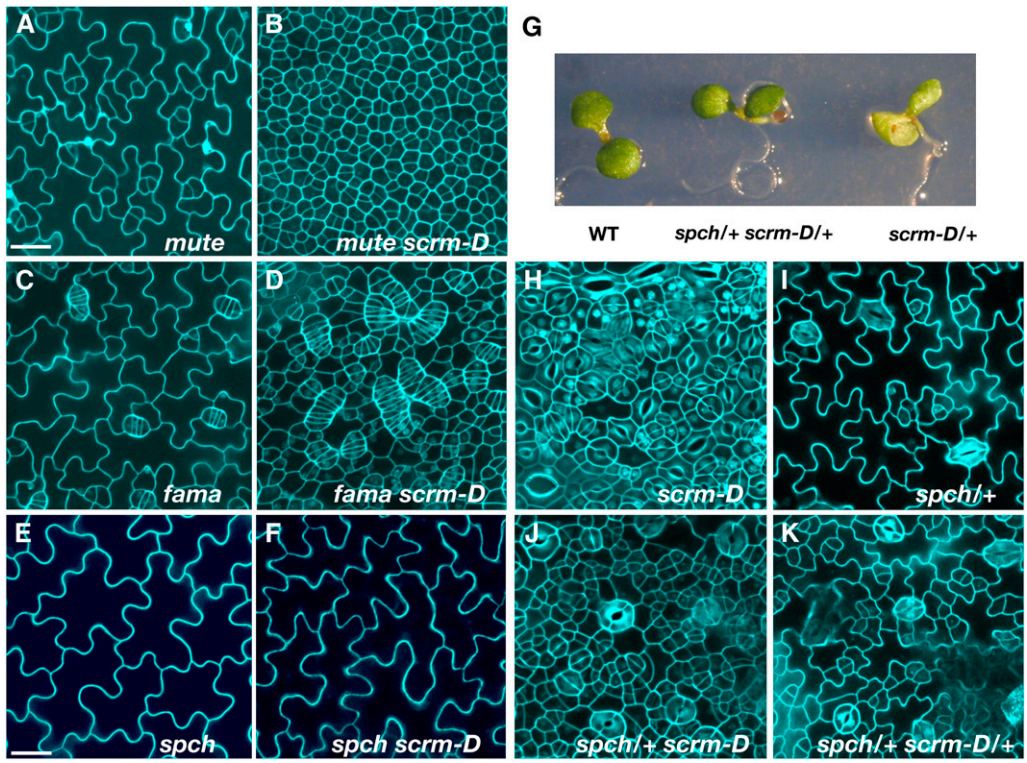

Figure 3. Genetic Interactions.

(A) to **(F)** Abaxial rosette leaf epidermis of *mute* **(A)**, *mute scrm-D* **(B)**, *fama* **(C)**, *fama scrm-D* **(D)**, *spch* **(E)**, and *spch scrm-D* **(F)**.
(G) Six-day-old seedlings of the wild type, *spch*/+ *scrm-D*/+, and *scrm-D*/+.
(H) to **(K)** Abaxial rosette leaf epidermis of *scrm-D* **(H)**, *spch*/+ **(I)**, *spch*/+ *scrm-D* **(J)**, and *spch*/+ *scrm-D*/+ **(K)**.
All images except for **(G)** were taken under the same magnification. Bars = 20 μm.

(Figure 3B). Likewise, *scrm-D* strongly enhanced the stacks of GMC-like cells seen in *fama* (Figures 3C and 3D). Therefore, *mute* and *fama* are epistatic to *scrm-D* with regard to stomatal differentiation, while *scrm-D* is sufficient to trigger ectopic formation of stomatal lineage cells in the absence of *MUTE* and *FAMA*. Combined, the results suggest that *SCRM* is upstream of *MUTE* and *FAMA*.

SPCH directs the first asymmetric division that establishes the stomatal cell lineage. In *spch*, all epidermal cells become pavement cells (MacAlister et al., 2007; Pillitteri et al., 2007). *spch scrm-D* double homozygous seedlings were phenotypically identical to *spch*, indicating that *spch* is epistatic to *scrm-D* (Figures 3E and 3F). While *spch* is a strict loss-of-function mutation and recessive on its own (Figure 3I; MacAlister et al., 2007; Pillitteri et al., 2007), heterozygous *spch*/+ suppressed the *scrm-D* phenotypes. The *spch*/+ *scrm-D* epidermis resembled that of *scrm-D*/+, and the *spch*/+ *scrm-D*/+ epidermis appeared nearly wild type (Figures 3H to 3K). Consistently, seedlings of *spch*/+ *scrm-D*/+ double heterozygous seedlings exhibited none of the characteristic wrinkled cotyledons seen in *scrm-D*/+ (Figure 3G; see Supplemental Figure 1 online). The suppression of *scrm-D* phenotypes by *spch*/+ indicates that there are dosage-dependent effects of *SPCH* on the *scrm-D* phenotype, suggesting the possibility that SPCH and SCRM gene products may act in molecular proximity.

SCRM Encodes a bHLH-Leucine Zipper Protein, ICE1

To gain insight into the molecular basis of *scrm-D* action, we identified the *SCRM* gene via a map-based approach (see Supplemental Figure 2 online). We found a G-to-A substitution in At3g26744/bHLH116, which encodes the bHLH-leucine zipper (bHLH-LZ) protein, ICE1 (Chinnusamy et al., 2003) (Figure 4). ICE1 is an upstream key transcriptional activator of the cold-induced transcriptome and freezing tolerance. The dominant *ice1* allele (hereafter called *ice1-1D*) was isolated for insensitivity to cold-induced reporter transcription. To our surprise, *ice1-1D* and *scrm-D* possess the exact same missense mutation that replaces Arg at amino acid 236 with His (R236H) (Figure 4A). Indeed, the epidermis of *ice1-1D* showed constitutive stomatal differentiation (Figure 4D). To confirm that the R236H mutation in ICE1 is sufficient to confer excessive stomatal differentiation, we introduced the *scrm-D* gene product ($ICE1_{R236H}$) driven by its own 2.5-kb promoter into wild-type plants. The transgenic

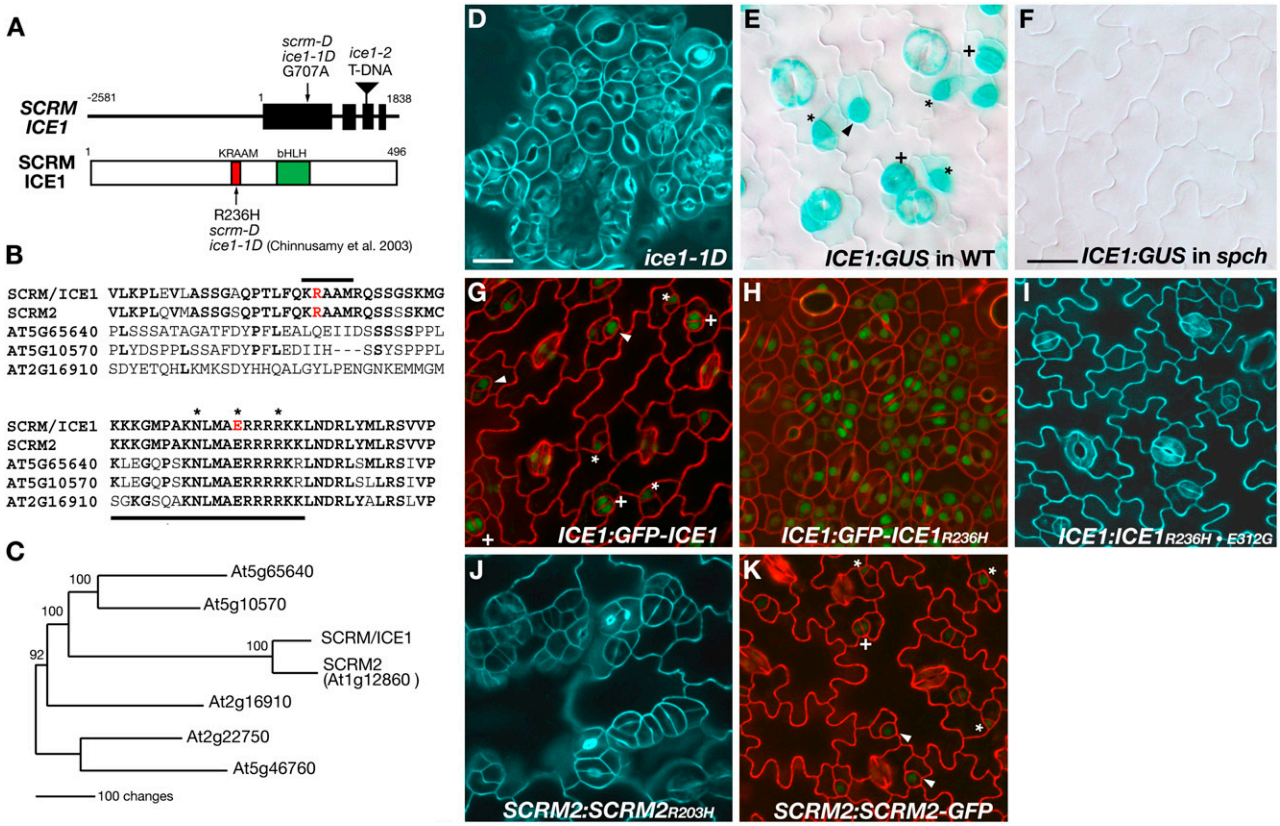

Figure 4. SCRM Is ICE1.

(A) *SCRM/ICE1* gene (top) and protein (bottom). Top: line, noncoding sequence; box, exon; triangle, T-DNA insertion. +1 corresponds to A at the initiation site (ATG). Bottom: 1 corresponds to the first Met at the initiation codon; red, KRAAM motif; green, bHLH domain. The locations of the mutation are indicated.

(B) Amino acid alignment of ICE1 and related bHLH proteins. Top: the KRAAM motif (marked by a solid line); red, the Arg residue substituted by His in scrm-D, ice1-1D, and SCRM2$_{R203H}$. Bottom: the basic region (underlined); red, the invariant Glu required for DNA binding; asterisks, core amino acid residues for DNA binding.

(C) Molecular phylogeny of ICE1 and related bHLHs. Shown is a parsimony tree based on the entire coding sequence (see alignment in Supplemental Data Set 1 online). Branch length reflects the number of amino acid changes. Bootstrap values (%) for 1000 replications are indicated on each node.

(D) Abaxial cotyledon epidermis of *ice1-1D*.

(E) *ICE1:GUS* expression (blue) in wild-type abaxial cotyledon epidermis.

(F) *ICE1:GUS* expression (blue) in *spch* abaxial cotyledon epidermis.

(G) Localization of GFP-ICE1 fusion protein (green) expressed by the native ICE1 promoter.

(H) Localization of GFP-ICE1$_{R236H}$ fusion protein (green) expressed by the native ICE1 promoter.

(I) Abaxial rosette leaf epidermis of *ICE1:ICE1$_{R236H•E312G}$*.

(J) Abaxial rosette leaf epidermis of *SCRM2:SCRM2$_{R203H}$* rosette leaves.

(K) Localization of SCRM2-GFP fusion protein (green) expressed by the native SCRM2 promoter.

For **(E)**, **(G)**, and **(K)**, meristemoids are indicated by asterisks, GMCs by arrowheads, and immature guard cells by plus signs. Bars = 20 μm.

seedlings expressing *ICE1:ICE1$_{R236H}$* recapitulated the *scrm-D*/+ phenotype, providing the evidence that *SCRM* is *ICE1*/*bHLH116* (see Supplemental Figure 3 online).

SCRM/ICE1 Is Expressed Broadly in Stomatal Cell Lineages

There is no previous report indicating a role of *ICE1* in stomatal differentiation. We thus examined its cellular expression patterns in the leaf epidermis. The *ICE1* promoter fused to the reporter *GUS* gene (*ICE1:GUS*) and GFP-ICE1 fusion protein (*ICE1:GFP-ICE1*) showed broad expression within stomatal cell lineages: strong expression in meristemoids and GMCs, moderate expression in immature guard cells, weaker expression in mature guard cells and surrounding SLGCs, and no expression in pavement cells (Figures 4E and 4G). The GFP-ICE1 fusion protein was nuclear localized, consistent with the function of ICE1 as a transcription factor (Figure 4G). No *ICE1* promoter activity was detected in the *spch* seedling epidermis, while *ICE1:GUS* expression outside of the stomatal cell lineage was unaffected by *spch* (Figure 4F; see Supplemental Figure 4 online). The

results support the genetic epistasis of *spch* to *scrm-D* and show that *SPCH* is required for stomatal lineage expression of *SCRM/ICE1.*

The *scrm-D* Point Mutation Confers a Gain of Function in *ICE1* and Its Paralog

To understand the functional significance of the *scrm-D* gene product, we next investigated the effects of the R-to-H substitution in ICE1. The functional fusion protein of scrm-D and GFP (ICE1:GFP-ICE1$_{R236H}$) resulted in nearly all epidermal cells differentiating into stomata and expressing GFP (Figure 4H). Similar to GFP-ICE1 (Figure 4G), GFP- ICE1$_{R236H}$ was detected solely in the nuclei (Figure 4H), suggesting that the *scrm-D* mutation does not affect subcellular localization. A second site mutation (E312G) that is known to destroy the DNA binding ability of bHLH proteins (Toledo-Ortiz et al., 2003) eliminated the phenotypic effects of the *scrm-D* mutation (Figure 4I), indicating that DNA binding is required for ectopic stomatal differentiation.

Based on phylogeny of the *Arabidopsis* bHLH gene superfamily, *ICE1* belongs to the bHLH subfamily 9, a subfamily distantly related to SPCH, MUTE, and FAMA (Toledo-Ortiz et al., 2003). Among the *ICE1* subfamily members, only the closest paralog, At1g12860/bHLH33, possesses a conserved stretch of amino acids (named a KRAAM motif) surrounding and including the Arg residue mutated in *scrm-D* (Figures 4B and 4C; see Supplemental Figure 5 online) (Toledo-Ortiz et al., 2003). To investigate the potential role of At1g12860/bHLH33 in stomatal differentiation, we first performed site-directed mutagenesis in At1g12860/bHLH33 to create an equivalent Arg-to-His substitution (R203H) and expressed the mutant gene driven by its own 3.8-kb promoter. The transgene conferred ectopic stomatal differentiation in the leaf epidermis (Figure 4J). Consequently, At1g12860/bHLH33 was named *SCRM2*. Our finding that SCRM2$_{R203H}$ phenocopied scrm-D (ICE1$_{R236H}$) highlights the gain-of-function nature of the mutation and the importance of the KRAAM motif in regulating stomatal differentiation.

We further examined the expression and localization patterns of SCRM2 to address its function during stomatal development. For this purpose, we generated transgenic *Arabidopsis* plants expressing SCRM2-GFP driven by its own promoter. Similar to ICE1, SCRM2-GFP fusion protein accumulated in the nuclei of stomatal precursors, notably in meristemoids, GMCs, and immature guard cells (Figure 4K). However, unlike GFP-ICE1, the SCRM2-GFP was not detected in mature guard cells. Our results indicate that *SCRM/ICE1* and *SCRM2* encode closely related, nuclear-localized bHLH proteins with largely overlapping expression patterns within the stomatal cell lineage.

ICE1 and *SCRM2* Specify the Three Key Transitional Steps to Form Stomata

To unequivocally address the role of *ICE1* and *SCRM2* during stomatal development, we investigated their loss-of-function phenotypes. For this purpose, T-DNA insertion alleles of *ICE1* (*ice1-2*) and *SCRM2* (*scrm2-1*) were characterized (Figure 5; see Supplemental Figures 5 to 7 online). In both lines, the T-DNA insertion led to absence (or substantial reduction) of the corresponding transcripts, indicating that they likely represent the null alleles (see Supplemental Figure 6 online; see Methods).

The *scrm2-1* single mutant showed no visible epidermal defects (Figure 5A). By contrast, the epidermis of *ice1-2* seedlings occasionally developed supernumerary GMC-like cells that were aligned in parallel, a phenotype resembling *fama* (Figure 5B). These rows of GMC-like cells occasionally differentiated a single, unpaired guard cell, which expressed the mature guard cell marker E994 (Figures 5B and 5C). Therefore, *ICE1* is required for fully restricting the number of GMC symmetric divisions and promoting proper terminal differentiation of guard cells.

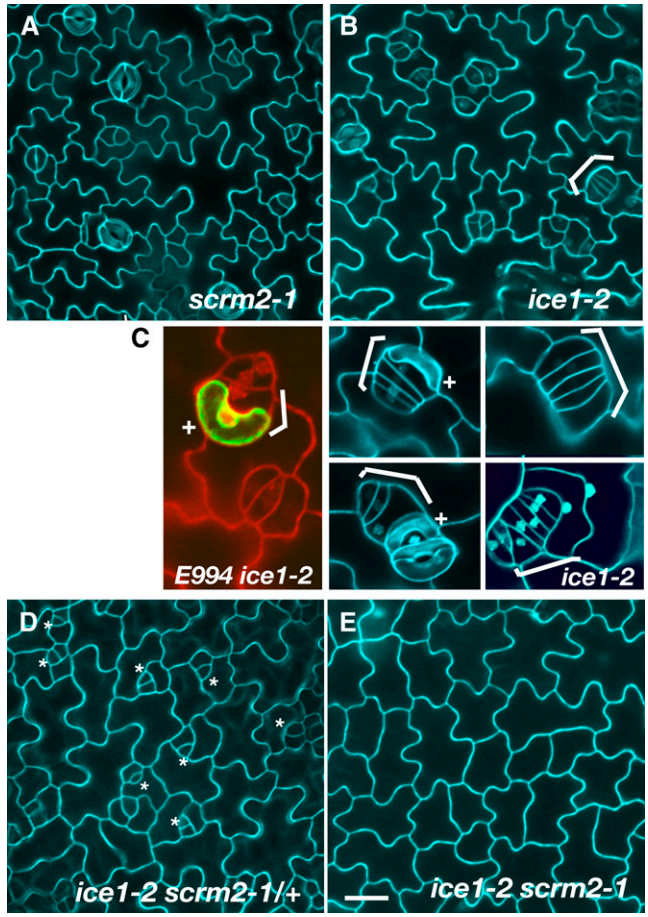

Figure 5. *ICE1* and *SCRM2* Are Required for the Successive Cell-State Transitional Steps Leading to Stomatal Differentiation.

(A) Abaxial rosette leaf epidermis of *scrm2-1*.
(B) Abaxial rosette leaf epidermis of *ice1-2*. Bracket indicates a GMC-like tumor.
(C) Close-ups of GMC-like tumors in *ice1-2* (brackets), showing occasional differentiation of single unpaired guard cells (+). Such an unpaired guard cell expresses the mature guard cell GFP marker, E994 (left panel).
(D) Abaxial rosette leaf epidermis of *ice1-2 scrm2-1*/+. Asterisks indicate arrested meristemoids.
(E) Abaxial rosette leaf epidermis of *ice1-2 scrm2-1.*
All images except for **(C)** were taken under the same magnification. Bar = 20 μm.

Strikingly, in the *ice1-2 scrm2-1*/+ epidermis, meristemoids arrested after rounds of amplifying asymmetric divisions, exhibiting a phenotype identical to *mute* (Figure 5D). Thus, in the absence of *ICE1*, *SCRM2* is haploinsufficient to drive the transition from meristemoid to GMC. Finally, the *ice1-2 scrm2-1* double loss-of-function mutants developed an epidermis made solely of pavement cells, a phenotype identical to *spch* (Figure 5E). Thus, *ICE1* and *SCRM2* redundantly direct the first asymmetric entry division that establishes stomatal cell lineage. Consistently, no *SPCH* transcripts were detected in *ice1-2 scrm2-1* (see Supplemental Figure 6 online). Introduction of wild-type *ICE1* and/or *SCRM2* genes via *Agrobacterium tumefaciens*–mediated transformation rescued these stomatal defects, providing the evidence that the phenotypes are due to their loss of functions (see Supplemental Figure 7 online). In summary, successive loss of *ICE1* and *SCRM2* recapitulates the phenotypes of *fama*, *mute*, and *spch*.

ICE1 and SCRM2 Form Heterodimers with Three Stomatal Key-Switch bHLHs

Our results suggest that ICE1 and SCRM2 are required for the sequential actions of SPCH, MUTE, and FAMA. To address if ICE1 and SCRM2 act as heterodimeric partners of SPCH, MUTE, and FAMA, we investigated their physical associations. First, we used a yeast two-hybrid system. Both ICE1 and scrm-D ($ICE1_{R236H}$) fused with the Gal4 DNA binding domain (BD: bait) showed strong transcriptional activation by themselves (Figure 6A). This is consistent with the previous report that both ICE1 and $ICE1_{R236H}$ strongly transactivate reporter expression in *Arabidopsis* (Chinnusamy et al., 2003). FAMA and SPCH fused with Gal4-DB alone showed very weak transcriptional activation, while MUTE did not show reporter activation (Figure 6A). We thus tested protein–protein interactions using MUTE, SPCH, and FAMA as bait and ICE1 and scrm-D ($ICE1_{R236H}$) as prey. Both

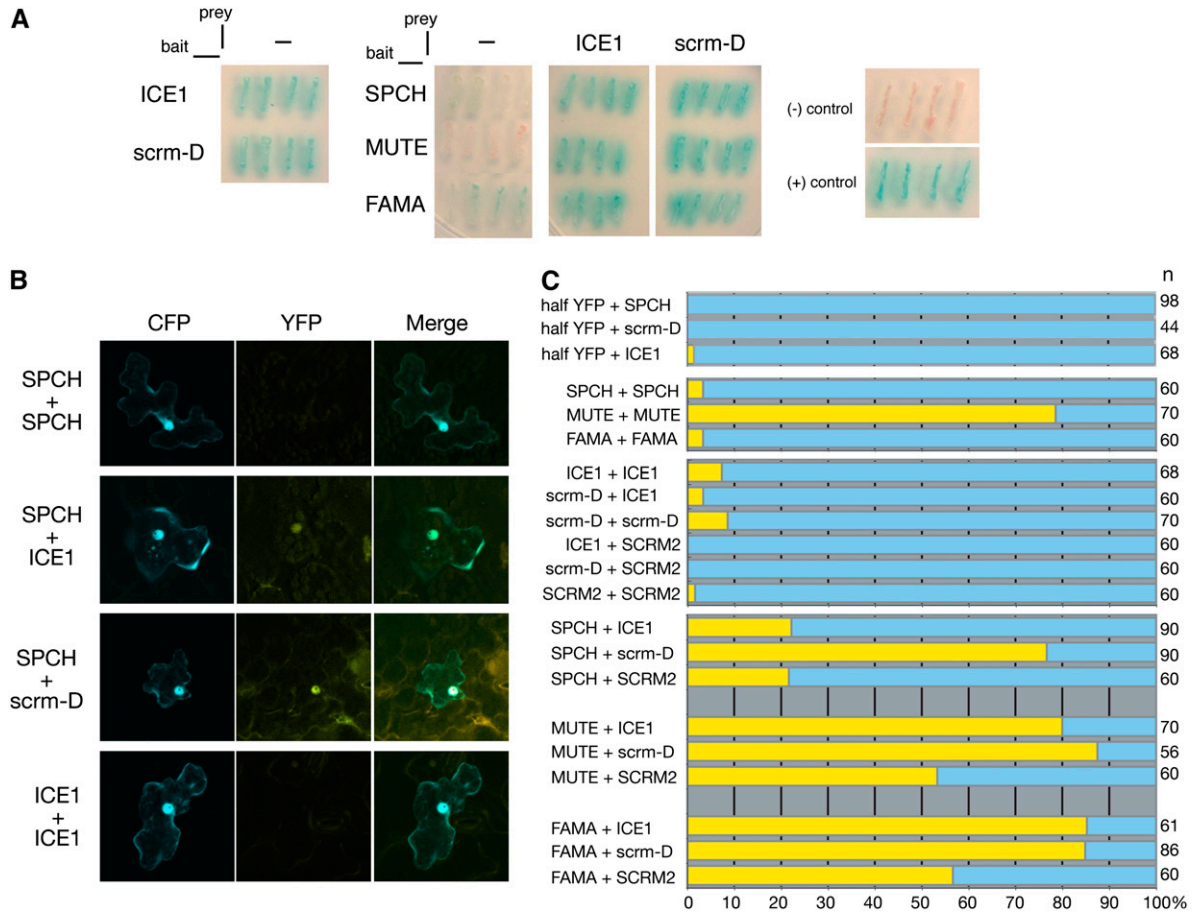

Figure 6. ICE1 and SCRM2 Associate with SPCH, MUTE, and FAMA.

(A) Yeast two-hybrid analysis. Blue indicates reporter activation. + and −, positive and negative controls of interaction, respectively.
(B) and **(C)** BiFC in the *Arabidopsis* epidermis.
(B) Representative confocal images of the BiFC analysis.
(C) Quantitative analysis. Left: pairwise combinations of bHLH constructs, each fused with a complementary, half-YFP molecule (left, nYFP fusion; right, cYFP fusion). Yellow bars represent percentage of cells expressing YFP (indicating molecular interactions) among total numbers of transformed cells (n).

ICE1 and scrm-D ($ICE1_{R236H}$) showed strong interaction with SPCH, MUTE, and FAMA (Figure 6A).

In the intact *Arabidopsis* epidermis using bimolecular fluorescent complementation (BiFC), ICE1, scrm-D ($ICE1_{R236H}$), and SCRM2 showed strong heterodimerization with MUTE and FAMA in the nuclei (Figures 6B and 6C). SPCH showed weaker association with ICE1 and SCRM2. However, scrm-D ($ICE1_{R236H}$) substitution enhanced its association with SPCH (Figures 6B and 6C). ICE1 family bHLH-LZ proteins did not associate with each other (Figures 6B and 6C). Likewise, SPCH and FAMA did not form homodimers, while MUTE did homodimerize (Figures 6B and 6C). The control combinations, including unfused half-yellow fluorescent protein (YFP) and ICE1, scrm-D ($ICE1_{R236H}$), or SPCH fused with complementary half-YFP, gave no signal, thus confirming the specific nature of the interactions (Figure 6C). The results suggest that the ICE1 family bHLH-LZs form core heterodimers with the stomatal-specific bHLHs. The reconstitution of complementary YFP molecules is influenced by multiple factors, and as such, the strength of YFP fluorescence in the BiFC system does not simply reflect the binding affinity of bHLH heterodimers (Lalonde et al., 2008). Nevertheless, we speculate that the R236H substitution might enhance in vivo heterodimerization with SPCH.

DISCUSSION

Through characterization of a dominant mutant, *scrm-D*, we made the surprising discovery that SCRM/ICE1 and its closely related paralog SCRM2 partner with SPCH-MUTE-FAMA bHLH proteins to drive the three steps of stomatal differentiation: initiation, meristemoid differentiation, and terminal differentiation of guard cells (Figure 7). It has been demonstrated that ICE1 binds to the Myc recognition sequence (CANNTG) (Chinnusamy et al., 2003). Because a functional DNA binding domain is required for the ectopic stomatal differentiation by the *scrm-D* gene product, $ICE1_{R236H}$, these nuclear-localized bHLH heterodimers most likely act as DNA binding transcription factors. Previously, two bHLH proteins, bHLH071 and bHLH093, were isolated as potential interactors of FAMA via a yeast two-hybrid screen (Ohashi-Ito and Bergmann, 2006). Their overexpression conferred a phenotype resembling a mild loss-of-function *fama* phenotype, suggesting that they negatively interfere with FAMA. It is worth mentioning that bHLH093 (At5g65640) belongs to the ICE1 family bHLH-LZs, although it lacks the KRAAM motif (Figure 4). Overexpression of bHLH093 (and also bHLH071) may have titrated out an available pool of FAMA from ICE1 and interfered with the formation of biologically functional ICE1-FAMA heterodimers. This scenario is plausible given that FAMA function is highly sensitive to a reduced dosage of ICE1 (Figure 5).

Our study highlights the intricate regulatory relationships between *SPCH* and *ICE1* for specifying an initial MMC population that gives rise to stomatal precursors. *SPCH* likely acts immediately upstream of *ICE1*, and *SPCH* is required to induce *ICE1* gene expression within the stomatal cell lineage (Figure 4). However, *ICE1* and *SCRM2* are required for *SPCH* expression and function, as the *ice1 scrm2* double loss-of-function mutant phenocopies *spch* with no detectable *SPCH* transcript accumulation (Figure 5; see Supplemental Figure 6 online). It has been reported that *SPCH* is initially expressed in the entire protoderm, but only a subset of SPCH-expressing cells initiate stomatal cell lineages (MacAlister et al., 2007; Pillitteri et al., 2007). Therefore, *SPCH* likely confers the competency to protodermal cells, but other factor(s) are required for the commitment of stomatal differentiation. ICE1 and SCRM2 are the best candidates for

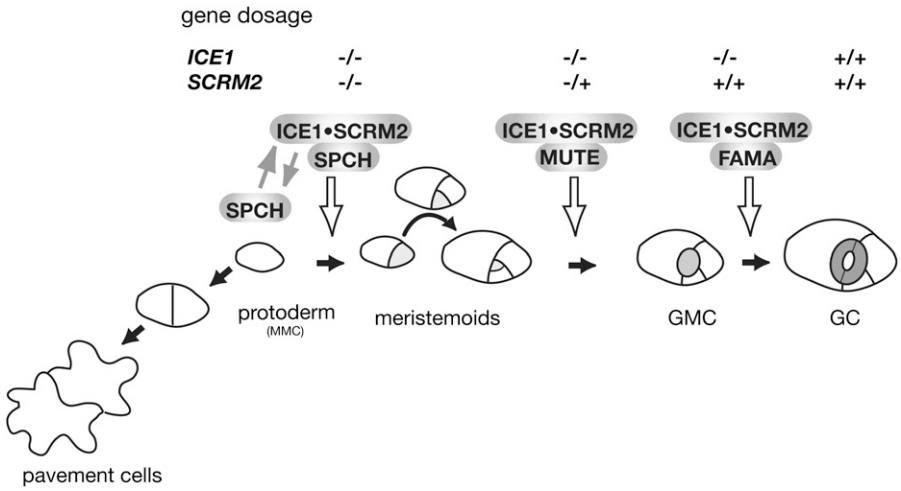

Figure 7. Models of Stomatal Cell-State Transition by Sequential Actions of bHLH Core Regulatory Units.

Schematic diagram of *ICE1* and *SCRM2* actions during stomatal differentiation. Both SPCH and *ICE1•SCRM2* are required for the first asymmetric cell division that initiates stomatal cell lineage. SPCH and ICE1•SCRM2 may influence each other's expression via a positive feedback (gray arrows). ICE1 and SCRM2 heterodimerize with SPCH, MUTE, and FAMA to direct initiation, meristemoid differentiation, and terminal guard cell differentiation, respectively (white arrows). The greater the loss of functional *ICE1* and *SCRM2* copies, the earlier the step of arrest during sequential, stomatal cell-state transition. +, functional gene copy; −, absence of functional gene copy by knockout mutation.

such factors. Based on this scenario, *SPCH* and *ICE1•SCRM2* influence each other's expression, and a positive feedback between *SPCH* and *ICE1•SCRM2* establishes the initial stomatal cell lineage. Subsequently, SPCH and ICE1•SCRM2 heterodimers direct asymmetric cell division that creates a meristemoid (Figure 7). This hypothesis is in accordance with the "stomata only" epidermal phenotype of *scrm-D*. The *scrm-D* mutation may stabilize SPCH activity in the entire protoderm. This may lead to the constitutive activation of SPCH via positive feedback and lock in all epidermal cells to adopt stomatal cell fate.

Our study establishes the core regulatory units of stomatal differentiation. Furthermore, the mechanism of SPCH-MUTE-FAMA specification by ICE1 and SCRM2 highlights the striking parallel in the molecular logic of cell-type differentiation between plants and animals (Pillitteri and Torii, 2007). For instance, skeletal muscle differentiation is directed by the sequential actions of four myogenic bHLH proteins that are expressed in specific precursor states within the muscle cell lineage (Olson, 1990; Weintraub et al., 1991; Jan and Jan, 1993; Weintraub, 1993). These muscle-specific bHLHs act via forming heterodimers with the ubiquitously expressed E-family bHLH proteins, which regulate wide varieties of developmental processes and pathogenesis (Murre et al., 1989; Sun and Baltimore, 1991; Massari and Murre, 2000). Similarly, three stomatal bHLHs, SPCH, MUTE, and FAMA, that exhibit transient expression within a specific precursor state of the stomatal cell lineage function as heterodimers with broadly expressed ICE1. The dual role of ICE1 in transcriptional regulation of cold tolerance and stomatal differentiation may be a reflection of the key strategy of land plants to integrate environmental inputs and developmental programs.

METHODS

Plant Materials

Arabidopsis thaliana Columbia (Col) was used as the wild type. All mutants and transgenic lines are in the Col background. The *scrm-D* mutant was derived from ethyl methanesulfonate–mutagenized Col *gl1-2* population and backcrossed three times before analysis (Esch et al., 1994). *ice1-1D* and *ICE1:GUS* are as described previously (Chinnusamy et al., 2003). T-DNA insertion alleles of *ICE1* (*ice1-2*; Salk_003155) and *SCRM2* (*scrm2-1*; SAIL_808_B10) were obtained from SIGnAL (Salk Institute) and the ABRC (Alonso et al., 2003), respectively. In *ice1-2*, the T-DNA is inserted within the third exon. In *scrm2-1*, the T-DNA is inserted in the 5′ untranslated region. Detailed analysis of the 5′-end of *scrm2-1* mRNA revealed that *scrm2-1* transcripts contain a long chimeric 5′ untranslated region with extra ATG derived from the T-DNA sequence, which codes for a short open reading frame (see Supplemental Figures 5 and 6 online). Other stomatal mutants and transgenic plants, specifically *spch*, *mute*, *fama*, *ERL1:GUS*, *TMM:GUS*, *SPCH:GUS*, *MUTE:GUS*, *FAMA:GUS*, *TMM:GUS-GFP*, *SPCH:SPCH-GFP*, *MUTE:MUTE-GFP*, and *FAMA:FAMA-GFP*, were described previously (Nadeau and Sack, 2002a; Shpak et al., 2005; Ohashi-Ito and Bergmann, 2006; Pillitteri et al., 2007). For details of genotype analysis, see Supplemental Table 1 online.

Microscopy

Microscopy was done according to Pillitteri et al. (2007), except that the Zeiss LSM 510 META was used for confocal microscopy.

Map-Based Cloning of SCRM

Because *scrm-D* is a dominant mutant, plants with the wild-type phenotype were selected as candidate recombinants from F2 plants of *scrm-D* (Col) × Landsberg *erecta* (L*er*). Approximately 6000 F2 plants were used for mapping the *SCRM* locus. DNA markers were used to detect polymorphisms between Col-0 and L*er.* The markers (see Supplemental Table 2 online) were designed based on the information available in the Monsanto *Arabidopsis* Polymorphism and L*er* Sequence Collection (http://www.Arabidopsis.org/Cereon/index.jsp). For the primer sequences and amplified fragment sizes in Col and L*er*, see Supplemental Table 2 online.

Phylogenetic Analysis

The full-length amino acid sequences were aligned (see Supplemental Data Set 1 online) using the default settings of ClustalW (Thompson et al., 1994). Phylogenetic analysis (neighbor joining and parsimony) was done using the default settings of Paup* 4.0 (Sinauer Associates), with At5g46760 and At2g22750 as outgroup. Bootstrap values were calculated from 1000 replications.

Molecular Cloning and Generation of Transgenic Plants

See Supplemental Table 3 online for a list of plasmid constructs generated in this study and Supplemental Table 4 online for a list of primer DNA sequences for molecular cloning. The Gateway-based transformation vectors were provided by Tsuyoshi Nakagawa (Shimane University) (Nakagawa et al., 2007). Generation and selection of transgenic plants and their phenotypic analyses were done as described by Pillitteri et al. (2007).

Yeast Two-Hybrid Assay

Yeast two-hybrid assay was done using the Matchmaker3 system (Clontech). Bait and prey constructs were transformed into yeast strain AH109, and α-galactosidase activity was assayed according to the manufacturer's protocol. See Supplemental Tables 3 and 4 online for plasmid construction and primer DNA sequence.

BiFC

To generate constructs for Split-YFP, *SPCH*, *MUTE*, *FAMA*, *ICE1*, *scrm-D*, and *SCRM2* were cloned into either pE3136, which contains N-terminal 174–amino acid of EYFP protein (nYFP), or pE3130, which contains C-terminal 64–amino acid of EYFP protein (cYFP) (a kind gift of Stan Gelvin, Purdue University). See Supplemental Table 4 online for construct information. All constructs were transiently expressed in *Arabidopsis* rosette leaves as previously described with some modifications (Walter et al., 2004). Microcarriers were prepared with 100 ng of each experimental construct (nYFP-fused and cYFP-fused constructs) and 50 ng of cauliflower mosaic virus 35S promoter fused to enhanced cyan fluorescent protein (ECFP). These plasmids were mixed and coated on 1.0-μm gold particle and bombarded to 2-week-old *Arabidopsis* seedlings using a Bio-Rad PDS-100/He particle delivery system. Sixteen to twenty-four hours after bombardment, specimens were observed under the Zeiss LSM 510META confocal microscope to simultaneously capture CFP and YFP at 458 and 514 nm, respectively. A pairwise combination of two bHLH constructs, each fused with a complementary half-YFP, were cotransformed with a control full-length CFP construct. The efficacy of heterodimerization was assessed by the percentage of cells expressing YFP among total number of CFP-expressing cells.

RNA Extraction, RT-PCR, and RACE PCR

RNA extraction, RT-PCR, and gel electrophoresis were done according to Pillitteri et al. (2007). The 5′ rapid amplification of cDNA ends (RACE)

was performed with the GeneRacer kit (Invitrogen) following the manufacturer's instructions. The PCR conditions used for amplification were as follows. First PCR (95°C): 3 min (95°C, 15 s; 72°C, 60 s) × 10 (95°C, 15 s; 70°C, 60 s) × 10 with the forward primer from the kit and reverse primer listed in Supplemental Table 5 online. Second PCR (95°C): 3 min (95°C, 15 s; 55°C, 15 s; 70°C, 60 s) × 30, 70°C 3 min with the reverse nested primer (see Supplemental Table 5 online). The PCR products were cloned in pCR4 TOPO TA cloning vector (Invitrogen) and sequenced.

Accession Numbers

During the course of research, we discovered that *SCRM2* (At1g12860) is misannotated in The Arabidopsis Information Resource database (http://www.Arabidopsis.org). The correct *SCRM2* gene structure and sequence, confirmed by 5′ RACE, can be found in Supplemental Figure 5 online. The GenBank accession number for *SCRM2* mRNA is EU369670. Other published sequence data can be found in the Arabidopsis Genome Initiative or GenBank/EMBL databases under the following accession numbers: *TMM* (At1g80080/NM_106657), *ERL1* (At5g62230/NM_125617), *SPCH* (At5g53120.1/NM_124700), *MUTE* (At3g06120.1/NM_111487), *FAMA* (At3g24140.1/NM_113319), and *ICE1* (At3g26744.1/NM_113586).

Supplemental Data

The following materials are available in the online version of this article.

Supplemental Figure 1. Seedling Phenotypes of *scrm-D*/+ and *scrm-D*.

Supplemental Figure 2. Fine Mapping of the *scrm-D* Locus.

Supplemental Figure 3. Recapitulation of the *scrm-D* Phenotype by Introduction of ICE1:ICE1$_{R236H}$ to Wild-Type Plants.

Supplemental Figure 4. Effects of *spch* on *ICE1:GUS* Expression in Nonstomatal Cells/Tissues.

Supplemental Figure 5. Structure of *ICE1* and *SCRM2* Genes and *SCRM2* mRNA and Amino Acid Sequence.

Supplemental Figure 6. RT-PCR Analysis of *ICE1*, *SCRM2*, *SPCH*, *MUTE* , and *FAMA* Transcript Accumulation in Wild-Type, *ice1-2*, *scrm2-1*, *ice1-2 scrm2-1*/+, and *ice1-2 scrm2-1* Seedlings.

Supplemental Figure 7. Phenotypic Complementation of *ice1-2*, *ice1-2 scrm2-1*/+, and *ice1-2 scrm2-1* Mutant Phenotypes by *ICE1* and *SCRM2*.

Supplemental Table 1. List of Primers and Their DNA Sequence Used for Genotype Analysis.

Supplemental Table 2. List of Primers and Their DNA Sequence Used for Map-Based Cloning of *SCRM*.

Supplemental Table 3. List of Plasmids Constructed in This Study and Their Descriptions.

Supplemental Table 4. List of Primers and Their DNA Sequence Used for Plasmid Construction.

Supplemental Table 5. List of Primers and Their DNA Sequence Used for RT-PCR and 5′ RACE PCR Analysis.

Supplemental Data Set 1. Alignment Used for Phylogenetic Analysis of ICE1 and Related bHLH Proteins.

ACKNOWLEDGMENTS

We thank Tatsuo Kakimoto, Jennifer Nemhauser, David Parichy, and Zhenbiao Yang for commenting on the manuscript, Stan Gelvin and Jessie McAbee for the split-YFP system, Shannon Bemis, Jessica Waite, and Ryo Matsushima for assistance, Ryan Miller for phylogenetic analysis, Tsuyoshi Nakagawa for cloning vectors, ABRC and SIGnAL for T-DNA insertion mutants, Dominique Bergmann for ongoing discussion about stomatal development, and Tom Daniel and Werner Stuetzle for purchasing a biolistic gun. Y.Y. is a Japan Society for the Promotion of Science predoctoral fellow. This work was supported by grants from the National Institutes of Health (R01GM059138) to J.-K.Z, the National Science Foundation (IOB-0520548), the Department of Energy (DE-FG02-03ER15448), and initially by the Japan Science and Technology Agency CREST award to K.U.T.

Received May 20, 2008; revised June 26, 2008; accepted July 2, 2008; published July 18, 2008.

REFERENCES

Alonso, J.M., et al. (2003). Genome-wide insertional mutagenesis of *Arabidopsis thaliana.* Science **301:** 653–657.

Berger, D., and Altmann, T. (2000). A subtilisin-like serine protease involved in the regulation of stomatal density and distribution in *Arabidopsis thaliana*. Genes Dev. **14:** 1119–1131.

Bergmann, D.C., Lukowitz, W., and Somerville, C.R. (2004). Stomatal development and pattern controlled by a MAPKK kinase. Science **304:** 1494–1497.

Bergmann, D.C., and Sack, F.D. (2007). Stomatal development. Annu. Rev. Plant Biol. **58:** 163–181.

Chinnusamy, V., Ohta, M., Kanrar, S., Lee, B.H., Hong, X., Agarwal, M., and Zhu, J.K. (2003). ICE1: A regulator of cold-induced transcriptome and freezing tolerance in Arabidopsis. Genes Dev. **17:** 1043–1054.

Esch, J.J., Oppenheimer, D.G., and Marks, M.D. (1994). Characterization of a weak allele of the *GL1* gene of *Arabidopsis thaliana.* Plant Mol. Biol. **24:** 203–207.

Hara, K., Kajita, R., Torii, K.U., Bergmann, D.C., and Kakimoto, T. (2007). The secretory peptide gene EPF1 enforces the stomatal one-cell-spacing rule. Genes Dev. **21:** 1720–1725.

Jan, Y.N., and Jan, L.Y. (1993). HLH proteins, fly neurogenesis, and vertebrate myogenesis. Cell **75:** 827–830.

Lai, L.B., Nadeau, J.A., Lucas, J., Lee, E.K., Nakagawa, T., Zhao, L., Geisler, M., and Sack, F.D. (2005). The Arabidopsis R2R3 MYB proteins FOUR LIPS and MYB88 restrict divisions late in the stomatal cell lineage. Plant Cell **17:** 2754–2767.

Lalonde, S., Ehrhardt, D.W., Loqué, D., Chen, J., Rhee, S.Y., and Frommer, W.B. (2008). Molecular and cellular approaches for the detection of protein-protein interactions: Latest techniques and current limitations. Plant J. **53:** 610–635.

MacAlister, C.A., Ohashi-Ito, K., and Bergmann, D.C. (2007). Transcription factor control of asymmetric cell divisions that establish the stomatal lineage. Nature **445:** 537–540.

Massari, M.E., and Murre, C. (2000). Helix-loop-helix proteins: Regulators of transcription in eucaryotic organisms. Mol. Cell. Biol. **20:** 429–440.

Murre, C., McCaw, P.S., and Baltimore, D. (1989). A new DNA binding and dimerization motif in immunoglobulin enhancer binding, daughterless, MyoD, and myc proteins. Cell **56:** 777–783.

Nadeau, J.A., and Sack, F.D. (2002a). Control of stomatal distribution on the Arabidopsis leaf surface. Science **296:** 1697–1700.

Nadeau, J.A., and Sack, F.D. (2002b). Stomatal development in Arabidopsis. In The Arabidopsis Book, C.R. Somerville and E. M. Meyerowitz, eds (Rockville, MD: American Society of Plant

Biologists), doi/10.1199/tab.0066, http://www.aspb.org/publications/arabidopsis/.

Nakagawa, T., Kurose, T., Hino, T., Kawamukai, M., Niwa, N., Toyooka, K., Matsuoka, K., Jinbo, T., and Kimura, T. (2007). Development of series of gateway binary vectors, pGWBs, for realizing efficient construction of fusion genes for plant transformation. J. Biosci. Bioeng. **104:** 33–41.

Ohashi-Ito, K., and Bergmann, D.C. (2006). Arabidopsis FAMA controls the final proliferation/differentiation switch during stomatal development. Plant Cell **18:** 2493–2505.

Olson, E.N. (1990). MyoD family: A paradigm for development? Genes Dev. **4:** 1454–1461.

Pillitteri, L.J., Bogenschutz, N.L., and Torii, K.U. (2008). The bHLH protein, MUTE, controls differentiation of stomata and the hydathode pore in Arabidopsis. Plant Cell Physiol. **49:** 934–943.

Pillitteri, L.J., Sloan, D.B., Bogenschutz, N.L., and Torii, K.U. (2007). Termination of asymmetric cell division and differentiation of stomata. Nature **445:** 501–505.

Pillitteri, L.J., and Torii, K.U. (2007). Breaking the silence: Three bHLH proteins direct cell-fate decisions during stomatal development. Bioessays **29:** 861–870.

Shpak, E.D., McAbee, J.M., Pillitteri, L.J., and Torii, K.U. (2005). Stomatal patterning and differentiation by synergistic interactions of receptor kinases. Science **309:** 290–293.

Sun, X.H., and Baltimore, D. (1991). An inhibitory domain of E12 transcription factor prevents DNA binding in E12 homodimers but not in E12 heterodimers. Cell **64:** 459–470.

Thompson, J.D., Higgins, D.G., and Gibson, T.J. (1994). CLUSTAL W: Improving the sensitivity of progressive multiple sequence alignment through sequence weighting, position-specific gap penalties and weight matrix choice. Nucleic Acids Res. **22:** 4673–4680.

Toledo-Ortiz, G., Huq, E., and Quail, P.H. (2003). The Arabidopsis basic/helix-loop-helix transcription factor family. Plant Cell **15:** 1749–1770.

von Groll, U., Berger, D., and Altmann, T. (2002). The subtilisin-like serine protease SDD1 mediates cell-to-cell signaling during Arabidopsis stomatal development. Plant Cell **14:** 1527–1539.

Walter, M., Chaban, C., Schutze, K., Batistic, O., Weckermann, K., Nake, C., Blazevic, D., Grefen, C., Schumacher, K., Oecking, C., Harter, K., Kudla, J. (2004). Visualization of protein interactions in living plant cells using bimolecular fluorescence complemenation. Plant J. **40:** 428–438.

Wang, H., Ngwenyama, N., Liu, Y., Walker, J., and Zhang, S. (2007). Stomatal development and patterning are regulated by environmentally responsive mitogen-activated protein kinases in Arabidopsis. Plant Cell **19:** 63–73.

Weintraub, H. (1993). The MyoD family and myogenesis: Redundancy, networks, and thresholds. Cell **75:** 1241–1244.

Weintraub, H., et al. (1991). The *myoD* gene family: Nodal point during specification of the muscle cell lineage. Science **251:** 761–766.